Article

CATALYTIC CARBON DOTS FOR BACTERICIDAL ACTIVITY THROUGH ENHANCED REACTIVE OXYGEN SPECIES GENERATION

Xiaoling Hu[a], Boxuan Li[a], Yazhen Liu[a], Baojian Li[a], Ling Fang[b], Quan Zhou[b,] and Wenping Zhang[a,*]
[a]Peace Hospital Affiliated to Changzhi Medical College, 046000 Changzhi, Shanxi, China
[b]Nanjing Jiatong Micro-nano Technology Co., Ltd. 210000 Nanjing, Jiangsu, China

Recebido em 20/04/2023; aceito em 04/09/2023; publicado na web 06/11/2023

Owing to merging antibiotic resistance, the synthesis of novel antibacterial agents becomes increasingly important. Carbon dots (CDs) belong to a new class of carbon-based nanomaterials that have shown great potential in combating emerging and drug-resistant infections due to their unique optical properties, such as excellent biocompatibility and easy surface modification. Herein, light-treated CDs (LCDs) with enhanced antibacterial activity and low drug resistance were synthesized by using a simple one-pot hydrothermal method. LCDs can generate reactive oxygen species (ROS) under the light-emitting diode light, which kill two pathogenic bacteria, including methicillin-resistant *Staphylococcus aureus* (*S. aureus*) and *Escherichia coli* (*E. coli*). In addition, *in vitro* experiments show that the liquid crystal displays excellent biocompatibility. Due to the visible photo-oxidative activity, LCDs can be used as photodynamic therapy agents, providing efficient bactericidal activity. This study provides a simple way to modify CDs that lead to new properties.

Keywords: carbon dots; antibacterial activities; photodynamic therapy; biocompatibility.

INTRODUCTION

Bacterial resistance to antibiotics is considered a major problem in public health fields, making fighting infections more difficult.[1-3] Chemical drugs and antimicrobial drugs are the main clinical treatments for bacterial and viral diseases.[4] However, studies have shown that many chemical drugs exhibit specific biological toxicity that can destroy normal tissue cells, especially in children. Nanotechnology can serve as an antibacterial strategy to treat many infectious diseases.[5,6] Nanoparticles (NPs) have also been widely used in many medical applications such as biosensing, drug delivery, bioimaging, and antimicrobial therapy.[7-9] NP-based therapeutics can inhibit bacterial-induced infection by directly eliminating bacteria by inhibiting bacterial growth and proliferation.[10-12] Therefore, NP-based strategies exhibit great potential in combating infectious diseases induced by bacteria.

Among the abundant nanoparticle-based antibacterial agents, the properties of carbon dots (CDs) are revealed to possess small particle sizes of less than 10 nm, stable fluorescence properties, and great biocompatibility, which are beneficial for a wide range of clinical applications.[13-15] Over the past few years, CDs have emerged as one of the nanotechnologies for disease diagnosis, indicator monitoring, and disease treatment.[16] CDs in suspension can generate reactive oxygen species (ROS) upon photoexcitation.[17] This knowledge indicates that CDs are potential candidates for photodynamic therapy (PDT), by which light-excited compounds damage cells by generating ROS through energy or electron transfer to molecular oxygen. Moreover, we recently reported that CDs could eliminate cancer cells in a ROS-dependent manner after blue light exposure.[18,19] PDT can also target microbial pathogens, which is becoming increasingly important in light of emerging antibiotic resistance and the consequent reduction in the effectiveness of conventional treatments.[20-22] Until now, most carbon-based nanomaterials exhibit antimicrobial properties, including fullerenes, carbon nanotubes, and graphene,[23] however, the exploration of CDs in the antibacterial field has not been extensively studied.

In this work, we employed 365 nm light-emitting diodes (LEDs) to process blue-light CDs for short periods (Figure 1). Expectantly, light-treated CDs (LCDs) with extended visible light absorption were obtained. Absorption bands in the visible region occur after photo treatment, allowing efficient photooxidation and PDT using LED light. LCDs possess excellent water solubility, stability, and biosafety. Meanwhile, positively charged liquid crystal shows easily attach to negatively charged bacteria through electrostatic interactions, exhibiting broad-spectrum antibacterial activity, decreasing the risk of

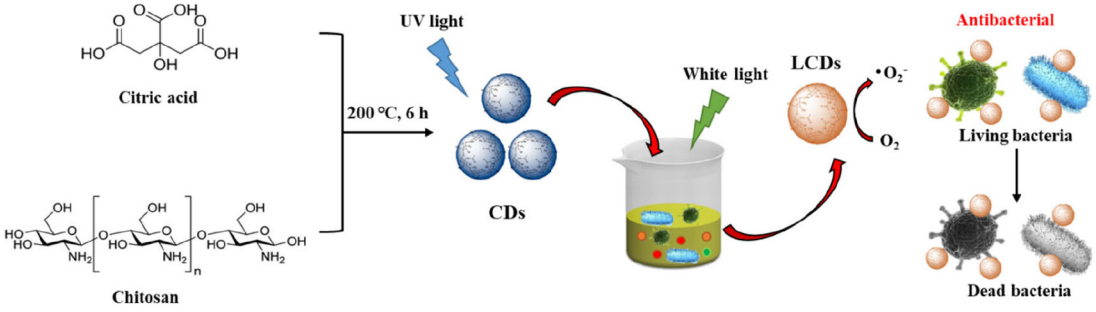

Figure 1. *Schematic illustration for synthesis and antibacterial properties of LCDs*

*e-mail: wenpingZhang1@126.com

drug resistance development. LCDs also show enhanced peroxidase (POD) and oxidase mimetic activity without light exposure. In addition, *in vivo* experiments show that LCDs have great antibacterial activity.

EXPERIMENTAL PART

Materials

All chemicals were used without further purification. Chitosan and 3,3',5,5'-tetramethylbenzidine (TMB) were purchased from Sigma-Aldrich (USA). Glycerol (>99%) and dimethyl sulfoxide (DMSO, >99.8%) were provided by Sangon Biotechnology (Shanghai, China). Dulbecco's modified Eagle's medium (DMEM) and fetal bovine serum (FBS) were purchased from Hyclone (USA). Milli-Q water was used in all experiments to prepare buffers and solutions.

Instrumentations

Diameter distribution and zeta potential were performed by Mastersizer2000 (DLS, Nano-ZS, Malvern, Instruments, Ltd., UK). Morphology and diameter were represented by transmission electron microscopy (TEM, Tecnai G, Spirit, FEI, Hong Kong). XRD pattern of the samples was obtained by an X-ray diffractometer (Ultima model, Rigaku Company) using monochromatic Cu-Kα radiation at room temperature. Electron spin resonance (ESR) measurement was made by using a JES-FA200 spectrometer from JEOL Ltd. (Tokyo, Japan). Superoxide of spin adduct BMPO/OOH was trapped by the 5-*tert*-butoxycarbonyl-5-methyl-1-pyrroline-*N*-oxide (BMPO) method.

Preparation of CDs

It was added 2 g of chitosan to 18 mL of 2% acetic acid solution and stirred at room temperature until homogeneous. Then, the mixture was sealed into a stainless steel autoclave filled with Teflon and placed in an oven at 180 °C for 12 h. Thereafter, the autoclave was cooled to ambient temperature and the obtained dark brown solution was centrifuged at 8000 rpm for 20 min to remove fewer fluorescent deposits. The solution was stored in the refrigerator for later use.

Light-treatment of LCDs

The above-prepared blue-emitting CDs (300 mg mL^{-1}, 1 mL) were added to a quartz colorimetric dish and irradiated by LED lights (365 nm, 3 W). The obtained LCDs with dark brown color were diluted and treated with freeze-drying for further characterization.[24]

POD-like activity of LCDs

The POD-like activity of LCDs contributed to the optimization of illumination time and pH. CDs were irradiated by LED lights (365 nm, 5 min) beforehead. Then, samples (PBS, only light, CDs, and LCDs) were treated with TMB and H_2O_2 to initiate the reaction. The absorbance of TMB at 652 nm was measured with a microplate reader (BioTek Instruments, USA).

Time-dependent TMB oxidation

Briefly, LCDs (250 μg mL^{-1}) were dispersed in 186 mL of acetate buffer (pH 4, 20 mmol L^{-1}), and then 4 mL TMB (40 mmol L^{-1}) and 10 mL H_2O_2 (20 mmol L^{-1}) were introduced to trigger the reaction. The absorbance of TMB at 652 nm was measured with a microplate reader.

In vitro cytotoxicity

HeLa cells were maintained in high glucose DMEM supplemented with 10% FBS and 1% penicillin/streptomycin at 37 °C in the presence of 5% CO_2. Cells were seeded in a 96-well plate at a density of 5×10^3 cells *per* well. After 24 h, the culture medium was replaced with 100 μL of fresh medium containing different concentrations of LCDs (0, 50, 100, 150, 200, and 250 μg mL^{-1}). The cell viability was measured by CCK8 assay. At the end of incubation, the cell culture medium was aspirated and supplemented with fresh medium followed by incubation with 10 μL of CCK8 *per* well for 3 h at 37 °C. The absorbance of solutions was monitored at 450 nm on a microplate reader.

Bacterial suspension and treatment

Before inoculation, the *S. aureus* and *E. coli* strains were transferred from the stock cultures to Columbia agar supplemented with 5% sheep blood and incubated aerobically at 37 °C overnight, followed by subcultivation under the same conditions. The cultures were then used for the preparation of bacterial suspensions in PBS. Then, 200 μL of bacterial suspension were transferred to a 15 mL tube, and 200 μL of LCDs (250 μg mL^{-1}) or PBS were added. After irradiation with LED (500 nm, 3 W), bacterial suspensions were centrifuged at 3000 rpm for 10 min and suspended in PBS for the determination of the antibacterial rate and ROS measurement. The detection of ROS was monitored by a fluorescence microscope (Olympus, Japan) under the excitation wavelength of 488 nm.

Dead bacteria staining

The preparation of the bacteria samples for dead bacteria staining was carried out according to the reported method. Exponentially growing *S. aureus* and *E. coli* were incubated overnight at 37 °C and centrifuged at 3000 rpm for 15 min, washed 3 times with PBS, and suspended in PBS to make a bacterial suspension with a concentration of 1.5×10^8 CFU mL^{-1}. Then, 900 μL of bacterial suspension and 100 μL of LCDs (0.5 mg mL^{-1}) were mixed in a sterile 1.5 mL tube. The tube was illuminated using LED (500 nm, 3 W) for 10 min after washing away the LCDs. The mixture was centrifuged at 3000 rpm for 15 min and suspended in 1 mL PBS after being washed 2-3 times with PBS. After that, 5 μL of propidium iodide (PI) solution (10 μmol L^{-1}) was incubated for 15 min in the dark. Finally, 2 μL of the sample was dropped on a confocal Petri dish and dried at 37 °C. The fluorescence imaging of 4',6-diamidino-2-phenylindole (DAPI) and PI were detected under the excitation wavelength of 405 nm and 561 nm, respectively.

Statistical analysis

The quantitative analyses in each experiment were shown as mean ± SD and *P* values were calculated by using the Student's two-sided *t*-test method.

RESULTS AND DISCUSSION

Characterization of LCDs

Firstly, the CDs-generated ROS under light illumination were synthesized, which exhibited potent photooxidation activity.

Moreover, the generated ROS could induce further crosslinking and oxidation of CDs, which would be a simple method to modify the CDs leading to new properties. The as-synthesized LCDs were characterized by TEM (Figures 2A and 2B). The TEM image showed the LCDs had monodisperse spherical morphology with an average size of 2.6 ± 0.3 nm. Meanwhile, the product yield of LCDs was 29.76 ± 3.13%. The HR-TEM images showed that LCDs possessed well-resolved lattice planes of 0.21 nm, consisting of the diffraction plane of (110) facet of graphite. The typical SAED pattern showed the LCDs are crystalline with a lattice fringe corresponding to the reported graphic CDs (Figure 2C). This *d*-spaces agrees well with the interplanar spacing of (002) diffraction facets of reported CDs with graphitic structure.[25] The crystalline nature of the as-prepared LCDs was further confirmed by XRD analysis (Figure 2D), which showed a broad peak because of the 002 Bragg reflection, showing good crystallization characteristics. The size distribution histograms of LCDs were obtained from the DLS analysis, which showed the diameter of LCDs were mainly distributed in the range of 2-4 nm, with an average diameter of 3.2 nm (Figure 2E), consistent with the TEM images. The zeta potential of LCDs was +14.85 ± 0.63 mV (Figure 2E), which indicated the surface of LCDs was positively charged. The size of LCDs did not change significantly during 21 days, indicating the stability of LCDs for long storage (Figure 2F).

Next, we used the POD-like activity of the LCDs to optimize the time of illumination and pH. The LED lights were used to treat CDs for 10 min, and then TMB and H_2O_2 were added to these samples. LCDs with LED light treatment could oxidize TMB into ox-TMB type in the presence of H_2O_2, which was identified by a significant absorption at 652 nm. As shown in Figure 3A, the absorbance of ox-TMB at 652 nm occurred a specific peak in the LED light-treated CDs group. This result suggested that LCDs exhibited better POD-like activity than CDs without LED light and single LED light. The time-dependent absorbance changes of TMB at 652 nm were displayed in Figure 3B, the absorbance of ox-TMB gradually increased with time. While the substrate concentration decreased with time, the catalytic activity reached a relatively stable value. Moreover, like other nanozymes, the catalytic activity of LCDs was tightly related to pH. The optimum pH at 4.0 indicated that the LCDs exhibited strong tolerance to harsh reaction conditions (Figure 3C). Expectedly, the POD-like activity of LCDs was detected to be highly active from pH 4 to 7, which was slightly different from the reported pH range of 3-4 required by POD mimetics. To verify the ability of LCDs in generating ROS, ESR spectroscopy was performed in aqueous solutions. Results showed that LCDs/LED lights were able to generate the signal of both superoxide anions (Figure 3D), indicating that superoxide anions could be mediated by LCDs after LED light irradiation.

Biocompatibility of LCDs *in vitro*

The biocompatibility of LCDs was investigated using HeLa cells. Figure 4A showed the viability of HeLa cells after incubating with LCDs in different concentrations. These results indicated that cell viability maintained over 90% under different concentrations of LCDs incubation and decreased with the increasing LCDs concentration, which confirmed the biocompatibility of LCDs in HeLa cells. In addition, the live/dead staining assay was performed to assess the viability of LCDs on HeLa cells after various treatments (Figure 4B). The green fluorescence predicted the live cells. There was no significant difference between the LCDs and the control group, which exhibited strong green fluorescence and further verified the excellent biocompatibility of LCDs.

Production of ROS by bacteria

As we described, the light-induced antibacterial effect of LCDs was a ROS-mediated photodynamic effect. To test this hypothesis, we measured intracellular ROS levels using DHR, a non-fluorescent indicator of cell permeability that could be oxidized to green fluorescent rhodamine. Fluorescent microscopy images showed that no ROS generation was observed in the control, single LCDs, or light group (Figure 5). In contrast, the amount of bacteria cells with green fluorescent ROS significantly increased in both *E. coli* and *S. aureus* suspensions after LCDs/LED light treatment. These results also suggested that neither single LCDs nor light could cause ROS-mediated oxidative stress. The antibacterial property of LCDs was initiated after disrupting the bacterial cell membrane and inducing a high level of ROS inside cells, which caused serious oxidative damage to bacteria proteins and nuclei acid, showing a higher antibacterial activity.

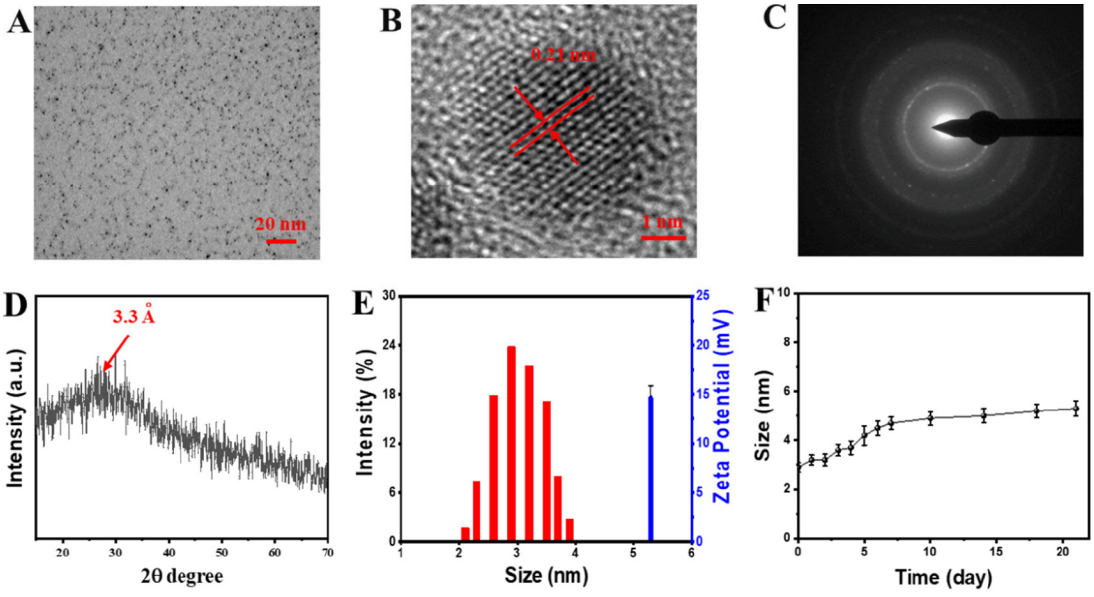

Figure 2. *(A) TEM and (B) HR-TEM images of LCDs; (C) typical SAED micro-graph of the LCDs; (D) XRD analysis of LCDs; (E) DLS and zeta potential of LCDs; (F) size change of LCDs stored in PBS for 21 days*

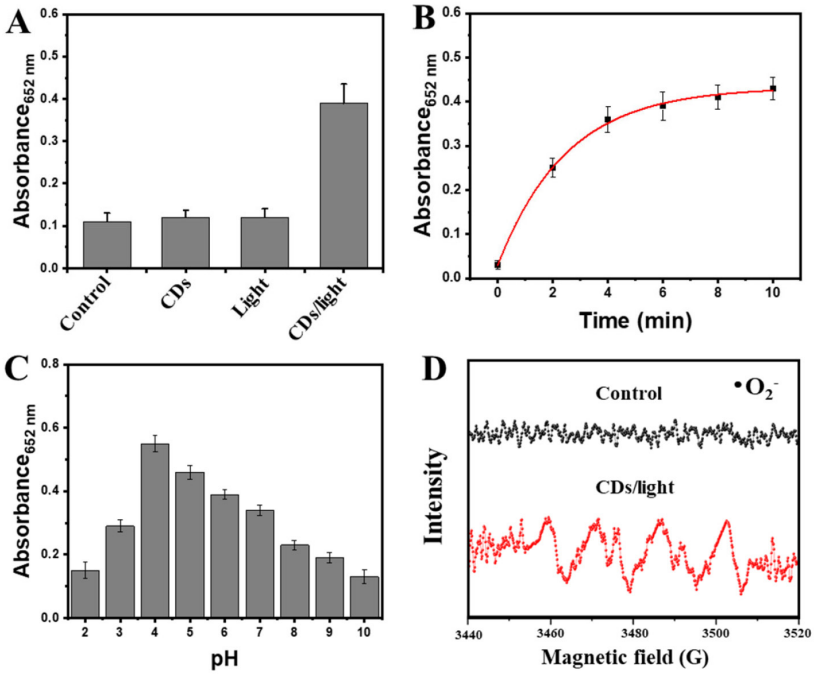

Figure 3. *(A) Absorbance of oxidation of TMB (0.8 mmol L^{-1}) by LED light-treated LCDs with H_2O_2 (1 mmol L^{-1}); (B) time-dependent absorbance changes of TMB (0.8 mmol L^{-1}) at 652 nm in the presence of LCDs with H_2O_2 (1 mmol L^{-1}); (C) absorbance of oxidation of TMB by LED light-treated LCDs processed at different pH; (D) ESR analysis of LED light-treated LCDs*

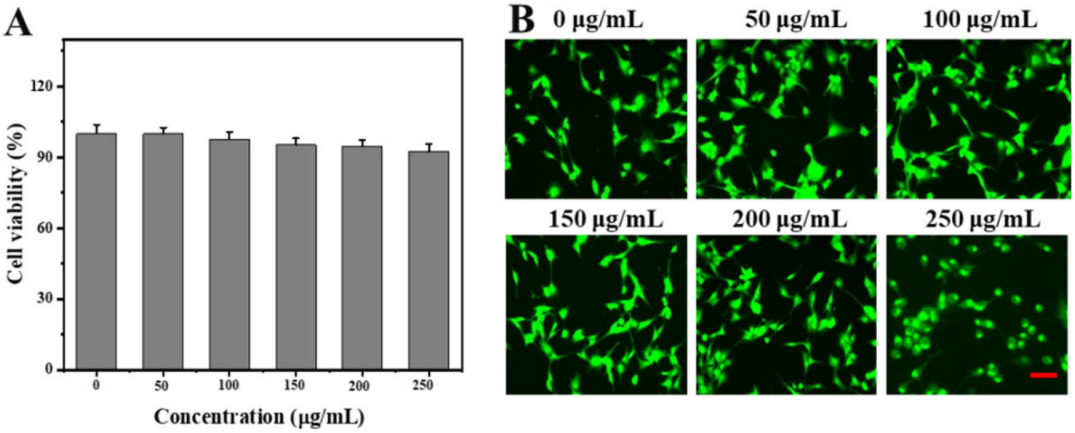

Figure 4. *(A) Viability of HeLa cells after LCD incubation at varying concentrations for 48 h; (B) live/dead staining of HeLa cells cultured with LCDs for 48 h (scale bar: 50 μm)*

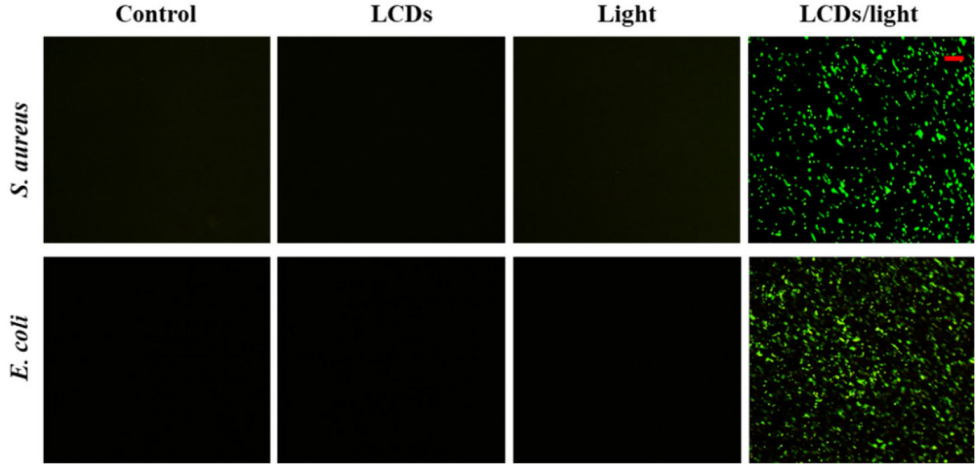

Figure 5. *Photoexcited LCDs induce oxidative stress in bacterial cells. Suspensions of E. coli and S. aureus were incubated with PBS or LCDs and exposed to LED light for 10 min. After staining with DHR, bacterial cells were visualized by fluorescence microscopy (scale bar: 10 μm)*

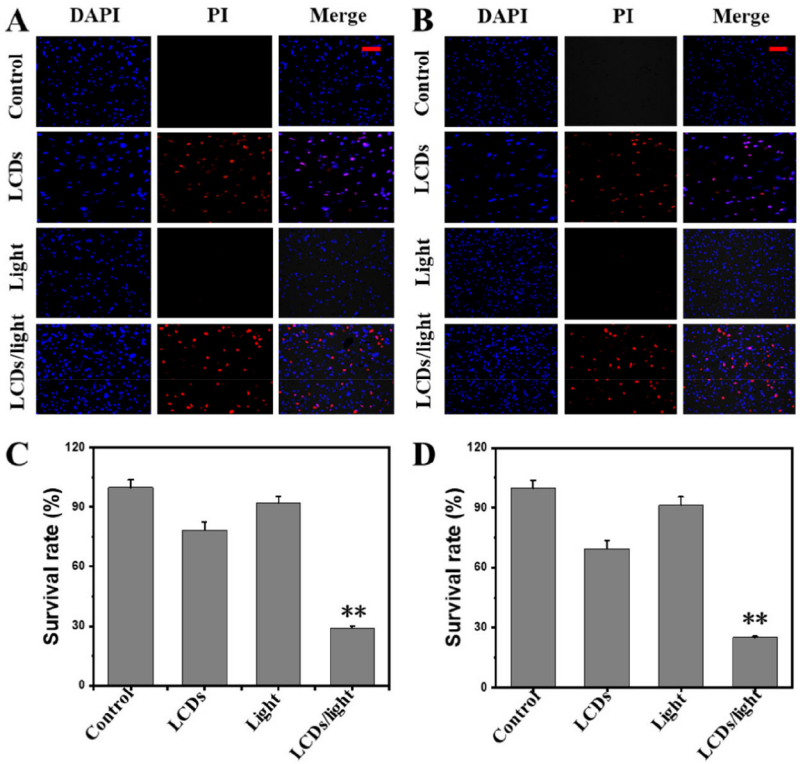

Figure 6. *Suspensions of (A) E. coli and (B) S. aureus were incubated with control (PBS), LCDs, light, and LCDs/LED light for 10 min. After staining with PI and DAPI, bacterial cells were visualized by fluorescence microscope. Scale bar: 10 μm. The survival rate of (C) E. coli and (D) S. aureus was determined by the standard plate count method. The data are mean ± SD values from a representative of three independent experiments (**p < 0.01)*

Antibacterial effect of LCDs

The antibacterial effect of LCDs was assessed using a fluorescence assay for cell membrane integrity, and the standard plate count method.[26,27] PI staining demonstrated that the maximal duration (10 min) of LED light exposure did not significantly affect the viability of *E. coli* (Figure 6A) or *S. aureus* (Figure 6B) as there was no red fluorescence. However, bacterial cells with LCDs at the highest concentration (200 μg mL^{-1}) treatment showed red fluorescence, which meant some dead bacteria appeared. However, bacteria with LCDs/light treatment exhibited a substantial loss in viability, as suggested by the increased red fluorescence in the number of PI-permeable bacteria. In agreement with the fluorescence-based assessment of cell membrane damage,[28] the plate count method also demonstrated a significant reduction in the number of CFU in both *E. coli* (Figure 6C) and *S. aureus* (Figure 6D) suspensions exposed to photoexcited LCDs. Therefore, it was inferred that photoexcited LCDs could efficiently destroy bacteria by generating ROS.

CONCLUSIONS

In summary, the data present here suggests that LCDs have relatively selective photodynamic antimicrobial activity. The *in vitro* experimental results show that LCDs have excellent biocompatibility. During LED light irradiation, ROS production induced the death of gram-negative bacteria *E. coli* and gram-positive *S. aureus*. Notably, these positively charged LCDs disrupt the permeability and integrity of bacterial plasma membranes more efficiently than conventional LCDs, resulting in significant inhibition of *S. aureus* and *E. coli* proliferation. These findings suggest that, as LED-triggered phototherapeutic nanomaterials, LCDs can foster the development of carbon nanomaterial-based treatments for bacterial infections. We identify that LCDs are suitable for wound healing treatments and display great potential in biomedical applications.

ACKNOWLEDGEMENTS

This work was supported by the Peace Hospital Affiliated with Changzhi Medical College and Nanjing Jiatong Micro-nano Technology Co., Ltd.

REFERENCES

1. Gao, Y.; Wang, W.; Mohammadniaei, M.; Zhang, M.; Shen, J.; Zhou, N.; *Appl. Catal., B* **2023**, *325*, 122314. [Crossref]
2. Ayaz, M.; Ullah, F.; Sadiq, A.; Ullah, F.; Ovais, M.; Ahmed, J.; Devkota, H. P.; *Chem.-Biol. Interact.* **2019**, *308*, 294. [Crossref]
3. Sánchez-López, E.; Gomes, D.; Esteruelas, G.; Bonilla, L.; Lopez-Machado, A. L.; Galindo, R.; Souto, E. B.; *Nanomaterials* **2020**, *10*, 292. [Crossref]
4. Pareek, V.; Gupta, R.; Panwar, J.; *Mater. Sci. Eng., C* **2018**, *90*, 739. [Crossref]
5. Wang, Y.; Yang, Y.; Shi, Y.; Song, H.; Yu, C.; *Adv. Mater.* **2020**, *32*, 1904106. [Crossref]
6. Yin, T.; Diao, Z.; Blum, N. T.; Qiu, L.; Ma, A.; Huang, P.; *Small* **2022**, *18*, 2104643. [Crossref]
7. Zhang, M.; Jiang, X.; Zhang, Q.; Zheng, T.; Mohammadniaei, M.; Wang, W.; Sun, Y.; *Adv. Funct. Mater.* **2021**, *31*, 2102274. [Crossref]
8. Bapat, R. A.; Chaubal, T. V.; Joshi, C. P.; Bapat, P. R.; Choudhury, H.; Pandey, M.; Kesharwani, P.; *Mater. Sci. Eng., C* **2018**, *91*, 881. [Crossref]
9. Wang, Y.; Chen, G.; Zhang, H.; Zhao, C.; Sun, L.; Zhao, Y.; *ACS Nano* **2021**, *15*, 5977. [Crossref]
10. Karaman, D. S.; Ercan, U. K.; Bakay, E.; Topaloğlu, N.; Rosenholm, J. M.; *Adv. Funct. Mater.* **2020**, *30*, 1908783. [Crossref]

11. Liu, S.; Cao, Y.; Ma, L.; Sun, J.; Ramos-Mucci, L.; Ma, Y.; Xiao, B.; *J. Controlled Release* **2022**, *347*, 544. [Crossref]
12. Li, W.; Wu, S.; Zhang, H.; Zhang, X.; Zhuang, J.; Hu, C.; Wang, X.; *Adv. Funct. Mater.* **2018**, *28*, 1804004. [Crossref]
13. Zhang, M.; Zheng, T.; Sheng, B.; Wu, F.; Zhang, Q.; Wang, W.; Sun, Y.; *Chem. Eng. J.* **2019**, *373*, 1054. [Crossref]
14. Zhang, M.; Yuan, P.; Zhou, N.; Su, Y.; Shao, M.; Chi, C.; *RSC Adv.* **2017**, *7*, 9347. [Crossref]
15. Wang, W.; Zhang, Q.; Zhang, M.; Liu, Y.; Shen, J.; Zhou, N.; Zhao, C.; *Analyst* **2020**, *145*, 3592. [Crossref]
16. Chung, S.; Revia, R. A.; Zhang, M.; *Adv. Mater.* **2021**, *33*, 1904362. [Crossref]
17. Ristic, B. Z.; Milenkovic, M. M.; Dakic, I. R.; Todorovic-Markovic, B. M.; Milosavljevic, M. S.; Budimir, M. D.; Trajkovic, V. S.; *Biomaterials* **2014**, *35*, 4428. [Crossref]
18. Markovic, Z. M.; Ristic, B. Z.; Arsikin, K. M.; Klisic, D. G.; Harhaji-Trajkovic, L. M.; Todorovic-Markovic, B. M.; Trajkovic, V. S.; *Biomaterials* **2012**, *33*, 7084. [Crossref]
19. Dong, X.; Ge, L.; Rabe, D. I. A.; Mohammed, O. O.; Wang, P.; Tang, Y.; Sun, Y. P.; *Carbon* **2020**, *170*, 137. [Crossref]
20. Pham, T. C.; Nguyen, V. N.; Choi, Y.; Lee, S.; Yoon, J.; *Chem. Rev.* **2021**, *121*, 13454. [Crossref]
21. Chen, J.; Fan, T.; Xie, Z.; Zeng, Q.; Xue, P.; Zheng, T.; Zhang, H.; *Biomaterials* **2020**, *237*, 119827. [Crossref]
22. Monro, S.; Colon, K. L.; Yin, H.; Roque III, J.; Konda, P.; Gujar, S.; McFarland, S. A.; *Chem. Rev.* **2018**, *119*, 797. [Crossref]
23. Cobos, M.; De-La-Pinta, I.; Quindós, G.; Fernández, M. J.; Fernández, M. D.; *Carbon* **2019**, *150*, 101. [Crossref]
24. Zhang, J.; Lin, Y.; Wu, S.; Hou, X.; Zheng, C.; Wu, P.; Liu, J.; *Carbon* **2021**, *182*, 537. [Crossref]
25. Dhanush, C.; Aravind, M. K.; Ashokkumar, B.; Sethuraman, M. G.; *J. Photochem. Photobiol., A* **2022**, *432*, 114097. [Crossref]
26. Higgins, D. L.; Chang, R.; Debabov, D. V.; Leung, J.; Wu, T.; Krause, K. M.; Humphrey, P. P.; *Antimicrob. Agents Chemother.* **2005**, *49*, 1127. [Crossref]
27. Wang, Z.; Bai, H.; Lu, C.; Hou, C.; Qiu, Y.; Zhang, P.; Mu, H.; *Carbohydr. Polym.* **2019**, *205*, 533. [Crossref]
28. Wang, W.; Wu, F.; Zhang, Q.; Zhou, N.; Zhang, M.; Zheng, T.; Tang, B. Z.; *ACS Nano* **2022**, *16*, 7961. [Crossref]